A Visual Analytics Tool for the Structural Health Monitoring of an Aircraft Panel

F. M. Pisano, M. Ciminello

Abstract—Aerospace, mechanical, and civil engineering infrastructures can take advantages from damage detection and identification strategies in terms of maintenance cost reduction and operational life improvements, as well for safety scopes. The challenge is to detect so called "barely visible impact damage" (BVID), due to low/medium energy impacts, that can progressively compromise the structure integrity. The occurrence of any local change in material properties, that can degrade the structure performance, is to be monitored using so called Structural Health Monitoring (SHM) systems, in charge of comparing the structure states before and after damage occurs. SHM seeks for any "anomalous" response collected by means of sensor networks and then analyzed using appropriate algorithms. Independently of the specific analysis approach adopted for structural damage detection and localization, textual reports, tables and graphs describing possible outlier coordinates and damage severity are usually provided as artifacts to be elaborated for information extraction about the current health conditions of the structure under investigation. Visual Analytics can support the processing of monitored measurements offering data navigation and exploration tools leveraging the native human capabilities of understanding images faster than texts and tables. Herein, a SHM system enrichment by integration of a Visual Analytics component is investigated. Analytical dashboards have been created by combining worksheets, so that a useful Visual Analytics tool is provided to structural analysts for exploring the structure health conditions examined by a Principal Component Analysis based algorithm.

Keywords—Interactive dashboards, optical fibers, structural health monitoring, visual analytics.

I. INTRODUCTION

MANY critical domains, such as aerospace, civil infrastructures, and automotive, take advantage from the utilization of composite materials, featured by their unique mechanical properties. Indeed, the combination of two or more different materials can result in a single composite material showing better performances than its constituting parts. On the other hand, damage could arise when those materials were subject to low/medium energy impacts. In this sense, in last decades the critical need of detecting possible damage at its early stage has come out in order to cope with maintenance reduction costs and, primarily, consequent safety issues. SHM aims at detecting, locating, and estimating damage in structures at the early occurrence in order to avoid unwanted failure. Typically, SHM systems collect, explore, and analyze data from structures in order to determine their

F.M. Pisano is with the Italian Aerospace Research Centre, Capua, CE 81043 IT (phone: +390823623591; e-mail: f.pisano@cira.it).

M. Ciminello is with the Italian Aerospace Research Centre, Capua, CE 81043 IT (phone: +39 0823623535; e-mail: m.ciminello@cira.it).

health status seeking for deviations from known nominal conditions.

Different types of sensors have been exploited in SHM. Recently, fiber-optic sensors (FOS) [1] have experienced widespread interest, because they are suitable to long cabling, that fits well to need of covering critical regions with higher risk of damage, for example, over aircraft surface. Optic fibers support high density of sensors collecting high volume of data though for short recording intervals, and assuring more reliable damage identification corresponding to positions uncovered by traditional sensors. It is worth underlining that damage detection is not as mature as strain sensing, so innovative algorithms to detect and locate damage from strain are to be conceived [2]. Data-driven methods aim at deriving damage information from structure strain response mapping by applying different loads: more significant information comes from sensors located close to the damage region and high-resolution sensor network is required. As an example, aircraft monitoring can need hundred meters of optic fiber, causing large strain measurement datasets to be analyzed and adequate algorithms are to be designed. PCA [3] is one of the most pervasive statistical techniques used for SHM. The main dynamics of a system can be identified by PCA, removing redundant or noisy data. This multivariate statistical technique can discover patterns and trends that would otherwise remain hidden in the data and reduce the size and complexity of data samples at the same time. In [4], the authors proposed a PCA-based algorithm for skin-stringer debonding detection and location using friendly box-and-whisker plots [5] to identify outliers. The algorithm was developed using the R statistical programming language [6].

Source data coming from the strain monitoring system and analytical algorithm outputs are typically provided as tables, leaving the domain expert bearing the burden of exploring and interpreting information about damage identification and localization. Effective presentation of hundred rows and columns of data can surely help in the task of inferring knowledge from tabular data following the Visual Analytics lifecycle depicted in Fig. 1.

SHM can take advantage from improved expressiveness of presented analysis results achieved applying Visual Analytics techniques. In [7], the combined PCA and box-plot algorithm outcomes have been integrated with the Visual Analytics approach to let domain experts navigate an image of the structural component under test, collecting information about occurrence and location of possible damage, corresponding to box-plot outliers, and significant strain statistical indices. Indeed, available information about the current health state of

the structure can be explored by users customizing the experience of investigating for patterns, trends, and correlations on their own. The VA application was developed using Tableau Desktop [8].
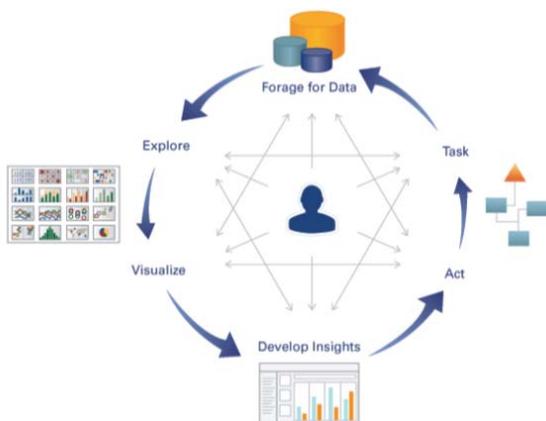

Fig. 1 Visual Analytics lifecycle [9]

In the present paper, more information is made available for navigation and exploration to the domain expert, integrating the collected strain data from the monitoring system within the interactive interfaces based on the structure image. In this way, the user can intuitively go further in the investigation of correlations and patterns connecting source and elaborated strain data.

II. STATE OF THE ART

Towards the end of nineties, a group of visionary researchers guessed the need of an innovative approach for data analytics to fill the gap between the existing Information Visualization capabilities and the increasing complexity of analytical needs emerging in the modern society.

A strong stimulus to innovative analytical solutions came from the dramatic 9/11 events, leading to government investments in the National Security domain. In such a context, the definition of Visual Analytics as "the science of analytical reasoning facilitated by interactive visual interfaces" was born in 2005 [10]. Visual Analytics is intended as a multidisciplinary research area [11]-[13], integrating Data Management and Analysis, Statistics, Spatio-temporal Data Processing, Visualization, and Human-machine Interaction, which aims at providing users innovative experiences in exploring and understanding information based on meaningful interactions through friendly interfaces.

The European Union started investing on VA for security and safety needs at the beginning of the 2000s as well [14]-[17].

A preliminary timeline of the VA development up to 2012 can be found in [18], highlighting the expected growth of VA domains and applications in subsequent years. In fact, VA applications have gone further in many different domains.

Healthcare is a critical domain featured by a number of variables that surpass the limits of human cognition. VA is regarded as a valuable key enabler for transforming the constantly growing health-related data in actionable knowledge [19]. A recent systematic scoping review of VA supporting mental healthcare systems is illustrated in [20]. Also, relevant commercial vendors as IBM, Tableau, and SAS offer solutions for healthcare [21]-[23].

Within the aviation safety domain, Boeing [24], [25] has investigated the issue of bird strikes over planes using VA to analyze the spatio-temporal distribution of incidents, which can cause severe damage in proportion of 1:20000 flights. Such a safety issue for aviation is also coped using VA methods and tools in [26].

An application of VA to a civil infrastructure as a bridge is discussed in [27] involving IBM Cognos* 8 business-intelligence software: visualizations of sensor data and analytics results support monitoring and interpretation of the bridge structure minimizing the required effort by allowing the drill down of summarized data. VA has been applied to SHM issues recently as well, still within the civil infrastructure monitoring: a preliminary approach using parallel axis plots of strains data collected by sensors located on a bridge is investigated in [28], illustrating the importance of visualization in understanding trends and patterns in data. Commercial products for the SHM of civil infrastructure have been created by Globvision [29], integrating data visualization capabilities as well. No VA application to the SHM for aircraft structure is known to the authors.

III. SHM SYSTEM ARCHITECTURE

In the present work, a Visual Analysis component is integrated within the SHM system composed by the structural specimen, the strain monitoring system and the PCA-based analysis algorithm as sketched in Fig. 2.

The proposed SHM system has been tested over an orthotropic carbon fiber, whose skin has a rectangular shape, 230 mm long (stringer direction), 350 mm wide and 4.5 mm thick. The skin's laminate is symmetrical and balanced with a total number of 24 plies. The panel has been subjected to a single 15 J impact, located at the center of the skin, to cause a "barely visible impact damage". Then the panel has been excited using an increasing load up to 800 N and the strains have been recorded by means of the fiber optic bonded along the stringer perimeters, as highlighted by the yellow line in Fig. 3. The fiber is 1 meter long and supports 731 sensors with an inter-distance of 2.6 mm; the system records strain measurements at 40 Hz frequency.

IV. SOURCE DATA

A. Data Understanding

The strain measurements of the current structure, recorded by the monitoring system, have been collected as a .xlsx file including a sheet containing 371 sensors as rows and 598 timestamps as columns. Gathered data from just one meter of optic fiber recording for less than 3 minutes exceed 2.5 MB. Then those measurements have been compared with the strains from the healthy structure using the PCA-based

algorithm [4], which provides a textual report, using Rmarkdown [30], and a .csv file containing some statistical indices, the discrepancies between the healthy and current

structure states projected onto a few selected principal components, and the outlier classification.
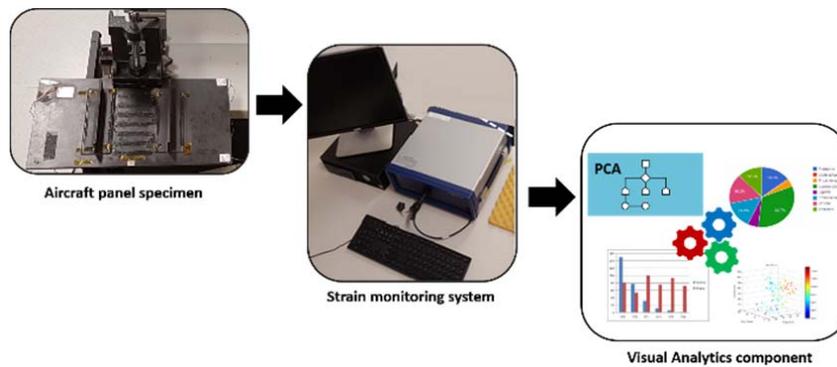
Fig. 2 SHM system architecture
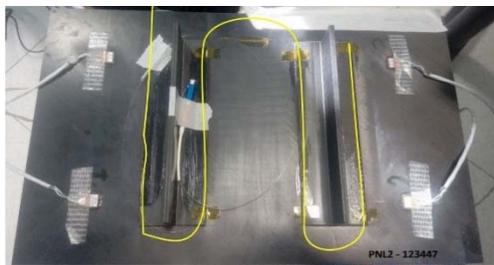
Fig. 3 Aircraft panel specimen with fiber optics bonded (yellow line)

B. Data Preparation

In order to set fiber optics sensor positions on the image of the aircraft panel specimen, the geo-reference of the sensors on the picture is needed. So, the coordinate system has been defined over the image and the specific sensor coordinates (x, y) have been calculated. An enriched .xlsx file of PCA-based analysis results is obtained adding two columns reporting the (x, y) coordinates of the sensor position. Moreover, monitoring data and elaborated analysis results have been combined in order to provide to the domain expert an integrated approach for information exploration and navigation. Source strain data are needed to be transformed from the matrix format to fields in a columnar table using the pivoting transformation, which replicates the sensor row for each value of timestamps; then geo-referenced coordinates of sensor positions can be added to the table. Besides, the custom data type for DateTime format including milliseconds, suitable for scientific data, has been defined over the timestamp column to get corresponding time series representation.

V. VISUAL ANALYTICS APPLICATION

A. Design

To design a VA application able to meet the user needs is fundamental to address some aspects well illustrated in [9], called "the seven essential elements of true visual analytics applications". The objective is to promote exploration, analysis, and collaboration beyond simple visualizations, by

offering querying, exploring, and visualizing as a single process. The human brain's ability to interpreter figures faster than text is leveraged by shifting and linking among different visualizations.

It is of fundamental importance to focus on audience's questions, answers to provide, and new potential emerging inspired questions. Each visualization has to suit a purpose and its content has to be selected coherently as the kind of charts as well. Within the charts, the most important information is recommended to be displayed over the x-y axes, the less important data can be integrated using shapes, color, and size. Another important aspect to be taken into account is avoiding information overloading in a visualization putting too many data in it; it is preferable to link among different visualizations so that the user can take advantage of the interconnected views profitably. Different charts can be combined in dashboards, in which the most relevant information is suggested to be available at the upper left corner, while charts to be filtered are better located at the bottom. No more than three or four charts in a single dashboard and presence of legends are considered as good design choices. More effectiveness of dashboards can be achieved using highlighting and filtering. Exhaustive guides to choose all the above listed elements can be found in [31], [32].

B. Tools

The geo-referencing of the aircraft panel picture in .jpg format has been realized using the Tableau Drawing Tool [33]. It is a web-based utility to allow to draw shapes on either user own images or on maps and then output the data for use in Tableau. Once the picture is loaded in the tool, the points corresponding to the beginning and the end of each of the four segments of the optic fiber along the four stringer caps is drawn and the associated coordinates are shown as a list that can be copied. Starting from the extreme points of each segment the coordinates of the remaining sensors can be derived using the known sensor inter-distance.

The VA application for supporting the SHM of the aircraft panel specimen has been developed using Tableau Desktop

[8], which is one of the most widespread Visual Analytics solutions worldwide. It is ranked as the second "Analytics and Business Intelligence Platform" for completeness of vision and ability to execute in the corresponding Gartner Magic Quadrant [34]. Tableau offers many graphs to be combined in effective worksheets including filters, highlights, legends and parameters and advanced features to create dashboards from them.

C. Worksheets

Primarily, the worksheet "Strain data table", in Fig. 4, reporting the 371x685 table of source monitored strain data is provided so that the user can start using the application from a very familiar display.

Strain data table

Sensor	201..	201..	201..	201..	201..	201..	201..	201..	201..	201..	201..	201..	201..	201..	201..	201..	201..	201..	201..	201..	201..	201..	201..	201..	201..	201..	201..	201..	20
229,9	-0,3	1,0	-0,7	0,1	-0,8	0,8	2,0	-1,7	-2,0	-2,1	1,1	-2,3	-0,6	-0,3	-0,5	1,8	0,5	1,0	-1,2	0,7	-1,2	-1,5	0,6	0,3	1,0	0,1	3,2	-0,2	1,1
232,5	0,9	1,2	-0,6	0,7	-0,4	0,8	1,1	-0,7	0,0	-1,3	1,1	-2,0	-0,3	-0,4	-0,5	2,2	1,3	1,0	-0,3	0,3	-0,9	-1,3	0,7	0,9	0,7	0,1	2,5	-0,4	0,4
235,1	1,8	1,9	-0,7	1,5	-0,1	1,3	0,8	-0,7	0,1	-0,4	0,9	-1,3	-0,3	0,4	0,0	2,3	1,8	1,1	1,3	0,2	-0,1	-0,8	0,8	0,5	1,1	1,1	3,2	0,8	0,4
237,7	1,5	1,6	-1,4	1,8	-1,0	-0,1	0,4	-0,4	-0,4	-1,8	-0,6	-2,0	-1,4	-0,5	0,7	1,4	0,4	0,9	0,6	0,3	-0,9	-1,2	0,5	-0,5	0,5	-0,2	2,7	0,0	-1,3
240,4	1,3	2,0	-0,9	1,5	-1,0	0,0	-0,6	0,0	-0,3	-0,4	-0,7	-1,4	-1,1	-0,6	-0,8	0,4	0,4	0,5	0,4	0,4	-0,7	-1,3	0,7	-0,2	1,5	0,3	1,9	-0,1	-0,5
243	1,7	0,9	-1,5	0,9	-1,2	0,3	-0,2	0,4	-0,3	-0,9	-0,4	-1,8	-1,0	-0,4	-1,3	1,2	-0,1	0,4	-0,4	-0,6	-0,6	-1,8	-0,3	-0,4	1,7	0,5	1,1	-0,3	-0,7
245,6	1,0	1,5	-1,3	1,7	-0,8	1,8	0,5	1,1	0,6	0,4	0,5	-0,5	-1,1	-0,1	-0,8	1,0	0,2	0,9	-0,9	-0,8	-0,2	-1,0	0,0	0,1	1,6	1,2	1,3	0,1	-0,9
248,2	0,2	0,1	-1,5	0,0	-1,1	0,3	-1,2	-0,7	-0,6	0,5	-0,5	-0,9	-1,5	-0,9	-1,5	-0,2	0,2	-0,1	-1,7	-1,5	-1,0	-2,1	-0,5	-0,1	0,7	0,5	0,9	-1,1	-1,1
250,8	-1,0	-0,4	-2,1	-0,7	-1,7	-0,5	-1,2	-1,6	-2,4	-0,3	-1,6	-1,7	-1,7	-1,4	-0,8	-0,8	-2,7	-1,3	-1,1	-2,6	-1,1	-1,1	1,1	-0,2	0,5	-1,6	-1,5		
253,4	0,4	0,6	-1,1	-0,4	-0,9	0,6	0,2	-1,0	-0,9	0,7	0,1	0,3	0,2	-0,5	-0,7	-0,2	0,3	0,4	-1,8	0,1	-0,2	-2,2	0,4	0,5	1,6	0,7	1,3	-0,2	0,2
256	1,6	0,2	-1,0	-0,5	-1,5	2,3	1,3	-0,3	-0,7	1,3	1,1	0,9	0,1	-0,5	0,2	0,3	0,9	0,5	-0,8	0,4	0,3	-1,7	1,0	0,9	2,7	1,6	1,6	0,8	1,0
258,6	1,6	-0,2	-1,4	-0,3	-1,5	2,6	2,4	0,0	0,1	1,4	2,1	0,9	0,7	-1,1	1,1	1,1	1,4	0,2	-0,9	0,7	0,3	-1,1	0,7	1,4	2,2	1,9	1,6	-0,8	0,7
261,3	0,2	0,1	-1,2	-0,1	-1,1	2,4	1,5	-1,6	1,3	1,4	2,3	1,2	-0,3	-1,6	1,2	0,4	1,5	0,8	0,0	1,5	-0,5	-0,6	1,7	1,1	1,0	0,6	1,4	-0,9	0,2
263,90..	0,9	0,3	-0,6	-1,2	-0,7	1,7	0,4	-2,4	1,3	1,5	1,0	0,7	1,1	-1,1	1,5	0,6	1,0	1,0	0,9	2,3	0,2	0,1	1,7	1,0	0,1	0,8	0,8	-2,2	0,9
266,5	-0,3	-1,0	-0,5	-1,2	-1,2	2,0	-0,4	-1,1	0,9	0,4	1,4	-0,5	-0,9	-1,3	0,7	-0,3	-0,8	0,5	-0,5	0,4	0,4	-1,0	0,8	0,0	-0,9	0,2	0,1	-2,1	-0,7
269,1	-0,1	-0,7	0,1	-0,7	-0,7	3,2	-0,1	0,2	1,7	2,0	1,4	0,2	-1,3	-0,4	1,0	-0,3	-0,2	1,7	0,7	1,3	0,8	0,2	1,1	1,1	-0,2	0,1	0,0	-1,2	0,3
271,7	-1,8	-1,9	-0,8	-2,0	-1,9	1,4	-2,6	-0,9	-0,3	-0,1	-0,9	-1,6	-2,7	-2,8	0,3	-0,8	-1,8	-0,8	-1,5	-1,1	-0,9	-1,0	-1,3	-0,8	-1,7	-1,1	-1,7	-2,8	-2,0
274,3	-1,8	-0,5	-0,6	-1,2	-0,8	1,1	-2,1	-0,3	1,1	0,6	-0,3	-1,2	-2,0	-1,8	0,2	-0,7	-1,4	-0,3	-1,3	-0,8	-0,3	-0,4	-0,7	0,0	-1,0	-0,5	-1,1	-2,4	-0,8
276,90..	-2,1	-0,8	-0,6	-1,4	-0,7	0,0	-2,0	-0,8	0,5	0,3	-0,7	-1,2	-1,4	-0,8	0,1	-1,1	-1,6	-0,8	-1,5	-1,2	-0,6	-0,4	-0,3	-0,5	-1,4	-1,2	-1,5	-2,7	-1,3
279,5	-1,5	-0,6	0,2	-1,4	-0,5	-0,2	-1,5	0,0	-0,2	0,5	-0,9	-1,1	-0,5	-1,2	-0,5	0,4	0,4	-1,0	0,8	0,0	-0,9	-1,2	-0,7	0,7	-1,2	-0,9	-1,3	-2,3	-1,3
282,2	-2,0	-1,4	-0,3	-1,8	-0,6	-0,6	-1,8	0,2	-1,0	-0,8	-0,6	-1,8	-1,3	-1,5	-0,2	-1,2	-2,0	-1,8	-1,1	-1,3	-0,7	0,1	-1,9	0,3					
284,8	-1,4	0,8	0,0	-0,9	0,3	-0,5	-1,1	1,1	0,0	0,4	-0,8	-1,2	0,3	-1,1	0,2	0,6	-0,7	-0,5	0,3	-0,2	0,4	1,0	-0,9	1,2					
287,40..	-1,1	1,6	0,9	-1,7	0,3	-0,6	-1,2	0,9	0,0	-0,5	1,0	-0,3	1,4	-1,1	0,7	1,7	-0,4	-1,1	-0,1	-0,7	0,2	0,1	-0,2	1,8					
290	-0,2	2,2	1,1	0,1	1,6	0,0	1,2	1,7	1,0	1,0	2,5	0,9	2,3	1,2	2,1	1,8	0,9	1,5	2,4	1,4	2,2	1,9	1,1	3,3					
292,6	-1,0	-0,2	0,9	-0,8	1,0	0,1	0,8	0,2	0,3	0,3	1,5	0,7	2,2	0,9	2,1	2,3	-0,2	1,2	1,2	0,6	0,8	1,3	1,1	1,8	0,4	-2,6	-1,1	-1,5	0,7
295,2	-0,3	-0,9	1,0	-1,2	0,9	0,5	1,2	0,1	0,3	-0,1	1,0	0,4	1,3	0,7	1,6	2,0	1,4	0,9	1,4	0,9	0,5	0,7	0,8	1,4	0,7	-1,5	-0,2	-2,1	1,5
297,8	-0,9	0,2	0,5	-0,6	1,1	1,6	1,1	0,1	1,0	0,5	1,3	1,0	1,1	1,3	1,3	2,2	1,0	1,4	1,1	0,5	0,8	1,1	1,5	0,9	1,5	-0,9	0,3	-2,0	2,1
300,40..	-0,4	0,4	1,0	-0,6	1,1	1,0	1,6	-0,2	1,7	1,2	0,7	1,3	0,8	1,8	1,3	2,1	1,7	1,9	0,9	0,8	0,7	1,2	1,8	0,7	1,2	-0,9	0,1	-2,0	2,0
303,1	-1,0	-1,2	0,5	-1,9	0,2	1,0	2,1	-0,5	0,8	0,7	0,3	1,7	0,2	1,6	0,6	1,6	1,0	0,9	0,1	0,7	-0,2	1,3	0,6	0,4	0,0	-1,0	-0,8	-2,0	1,8
305,7	-0,1	-1,3	0,5	-1,0	1,6	0,7	2,4	-0,1	0,7	0,9	-0,3	1,6	0,9	3,2	0,3	2,0	0,3	1,9	1,3	1,6	1,2	3,1	0,6	0,3	-0,5	-0,2	1,5	-1,2	3,1
308,3	-0,3	-1,5	-0,3	-1,7	0,7	0,5	0,9	-1,1	1,0	2,0	-1,6	1,5	0,3	2,7	-1,3	1,7	-0,5	1,0	-0,3	0,9	0,2	1,2	0,2	-0,3	-0,9	-1,1	0,8	-1,3	3,3
310,90..	0,1	0,6	1,1	-0,1	1,4	0,1	0,5	0,3	1,0	2,7	0,2	2,2	1,8	3,0	-0,1	1,8	0,8	1,6	1,1	1,6	1,8	1,9	0,3	1,2	0,3	1,7	2,9	0,0	3,4
313,5	0,0	0,8	0,3	-0,1	0,5	0,0	-1,2	0,3	0,6	2,0	0,1	1,2	0,9	1,5	-0,3	1,2	-1,7	1,7	0,1	0,1	0,4	1,7	0,5	0,9	0,2	0,2	1,7	0,5	1,6
316,1	-0,1	0,4	1,4	0,3	0,9	-1,7	-0,8	0,8	0,5	1,5	0,0	1,0	0,4	2,4	0,0	1,3	-1,4	2,1	0,7	0,9	0,2	1,0	1,2	0,8	-0,8	0,4	1,8	0,4	1,9
318,7	-0,2	0,4	1,9	1,0	1,6	-0,7	-0,9	1,1	0,7	1,2	0,8	1,1	0,7	2,2	0,9	1,2	-1,9	2,7	0,9	0,8	0,1	0,5	1,6	1,4	0,4	0,9	1,9	0,4	1,8

Tooltip: Timestamp: 2017-10-18 18:10:16.159 — Sensor: 276,900000000 — Strain (µε): -0,5

Tabs: Strain data table | Strain optic fiber | Strain sensor series | PNL2-123447 | Box-plot Diff1 | Box-plot Diff2 | Box-plot Diff3 | Diff1, Diff2, Diff3 | MAX, MEAN, MIN | DIFF1-2-3 | MAX MEAN MIN | Strai

Fig. 4 Strain data table worksheet

The subsequent two worksheets offer the representation of the recorded strain both along the whole fiber at different timestamps and for each sensor along the monitoring time interval. The worksheets have been named "Strain optic fiber" (Fig. 5) and "Strain sensor series". In the former worksheet, sensors are positioned as columns and strain data as rows and the specific timestamp is represented using a specific color as the legend on the right side indicates. Besides, filtering on timestamps is provided by choosing time interval on a scroll bar in the upper right corner. Moreover, highlighting of a specific timestamp that can be selected by clicking on the corresponding line on the chart and multiple selection can be set using the Ctrl button. Similarly, in the latter worksheet, timestamps are positioned as columns and strain data as rows and the specific sensor is represented using a specific color as the legend on the right indicates. Moreover, filtering on sensors is provided by ticking sensor IDs from a list on a scroll bar; highlighting of a specific sensor that can be selected by clicking on the corresponding line on the chart and multiple selection can be set using the Ctrl button.

The worksheet for the aircraft panel image navigation has been created selecting the picture as background from the Map menu in Tableau Desktop. The maximum and minimum values of the coordinates (x, y) have to be inserted as properties using the values elaborated by the Tableau Drawing Tool. Then the X, Y dimensions corresponding to the geo-referenced sensor coordinates are selected as columns and rows, respectively. The dimension related to sensor ID is inserted as textual information adding coordinates and outlier classification from the PCA algorithm. In this way, information about the sensor ID, its position and the damage evaluation are rapidly prompted moving the cursor over the image. Moreover, the outlier classification is introduced as filter, so that the user can easily visualize the location of possible damage setting the filter to the TRUE value, or the aircraft panel parts still healthy setting the filter to the FALSE value. In addition, the outlier classification is also shown using the red color for TRUE values and the green one for the FALSE values. The worksheet has been named as the panel code: PNL2-123447 (Fig. 6).

The differences between the healthy and current structure states projected onto the first three principal components and the maximum, mean, and minimum strain data are depicted in two separate worksheets "Diff1, Diff2, Diff3" (Fig. 7), "MAX, MEAN, MIN", using size to provide information about the outlier classification outcomes: bigger circles stand for TRUE values, smaller ones represent FALSE values. In addition, three worksheets "Box-plot Diff1", "Box-plot Diff2", "Box-

plot Diff3" representing the box-plots for differences between the healthy and current structure states projected onto the first three principal components are built, visualizing outlier classification outcomes using red and green colors.
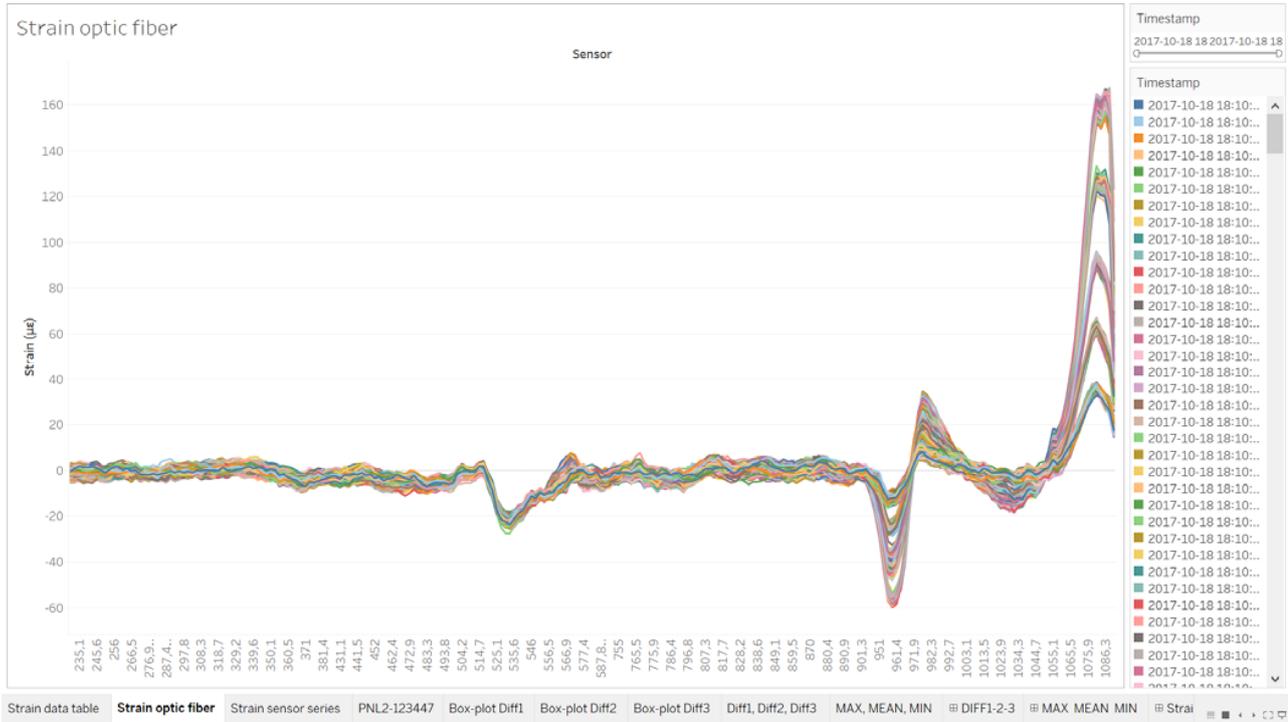

Fig. 5 Strain optic fiber worksheet
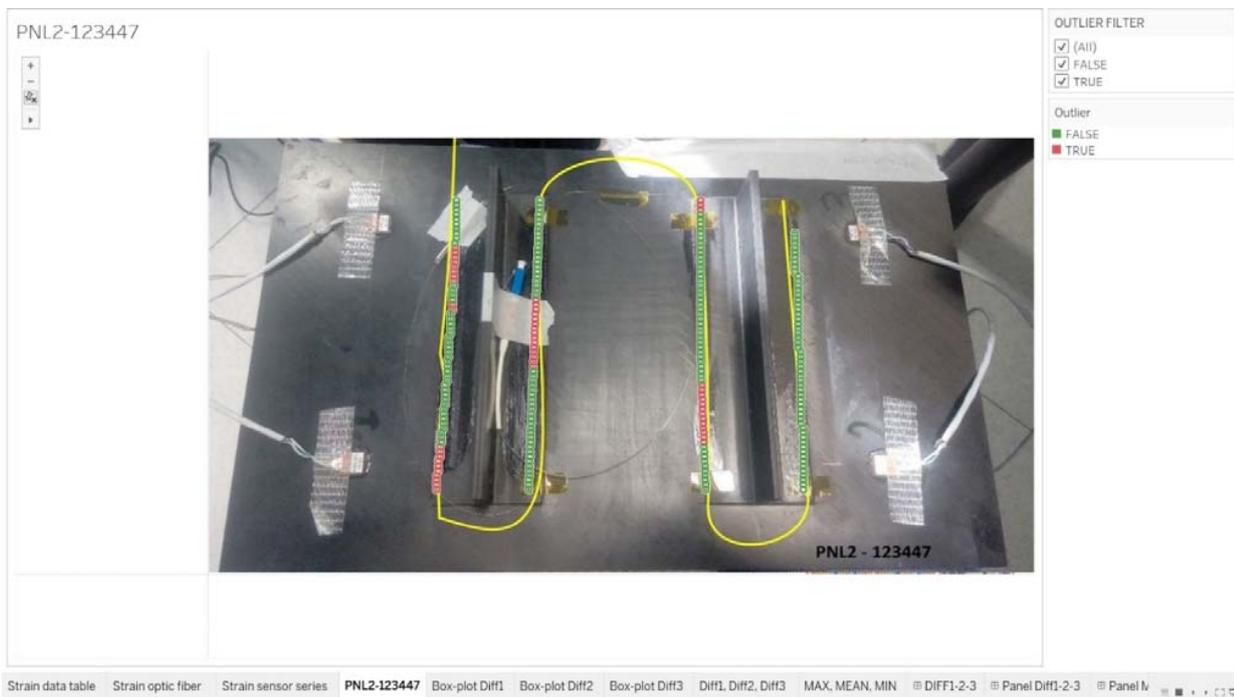
Fig. 6 Panel PNL2-123447 worksheet

Unfortunately, the integration of R scripts into Tableau is limited to aggregated measures so it was not possible to integrate into Tableau the parametric box-plot whiskers calculation as defined in [7]. Consequently, users can easily

verify that the PCA-based algorithm exploits stricter conditions over the outlier definition with respect to standard box-plots. Indeed, red points occurred between the standard lower and upper whiskers as well.
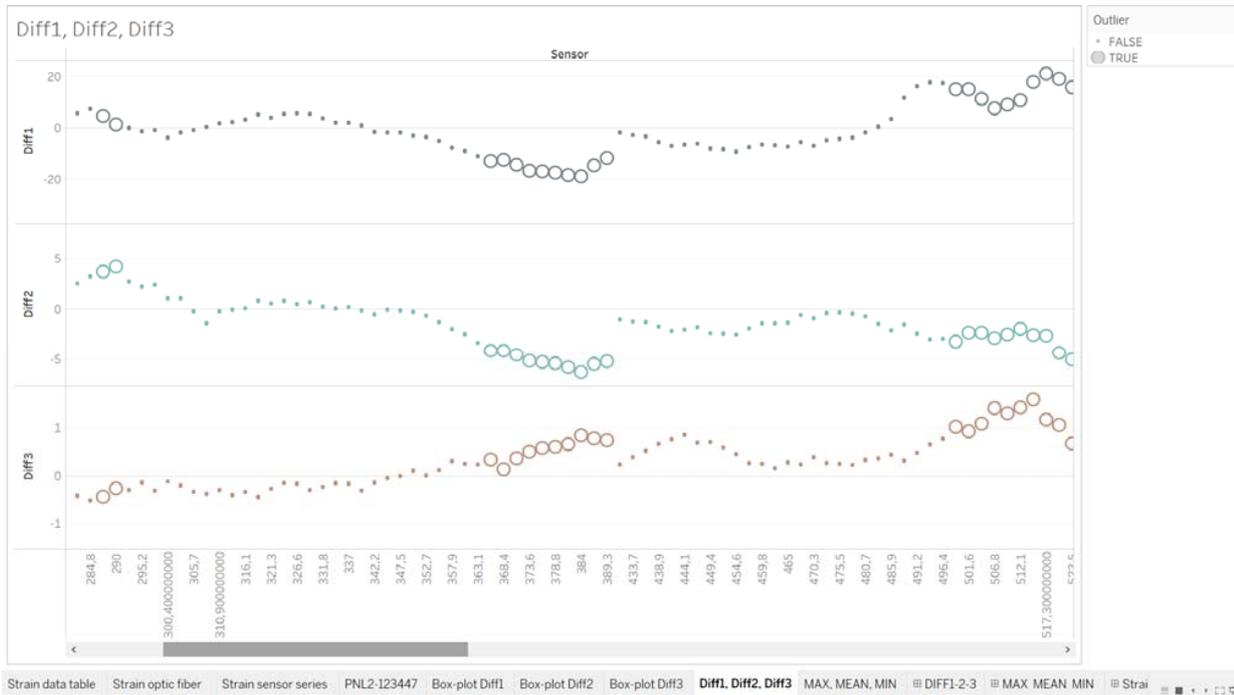
Fig. 7 Diff1, Diff2, Diff3 worksheet
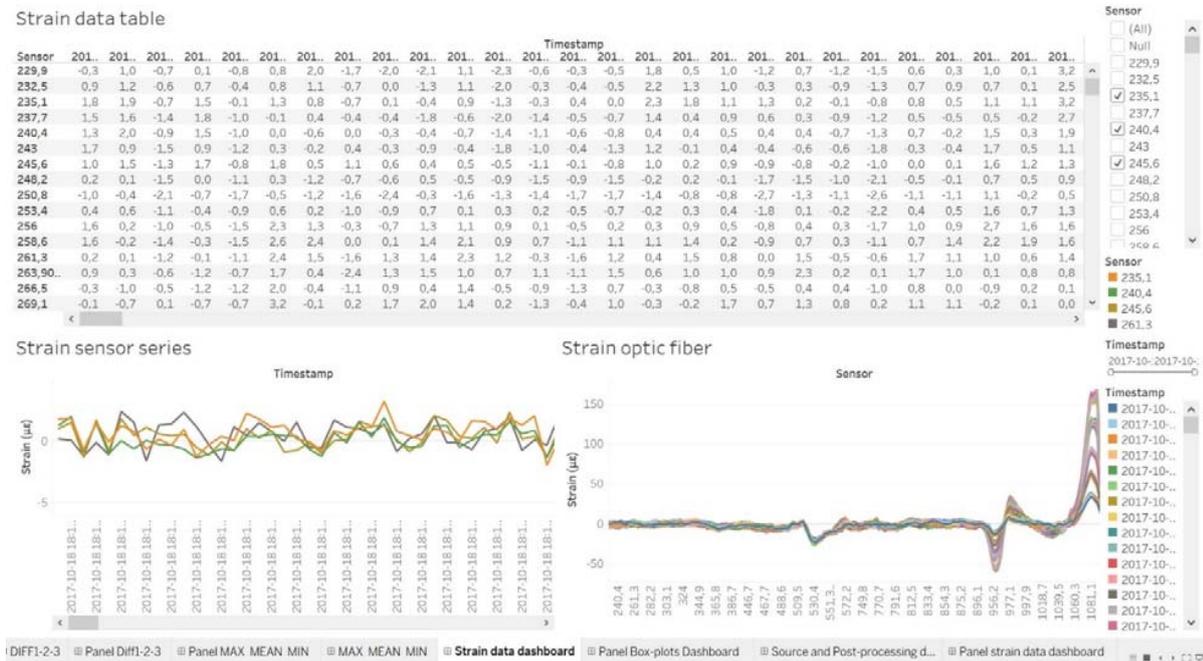
Fig. 8 Strain data dashboard
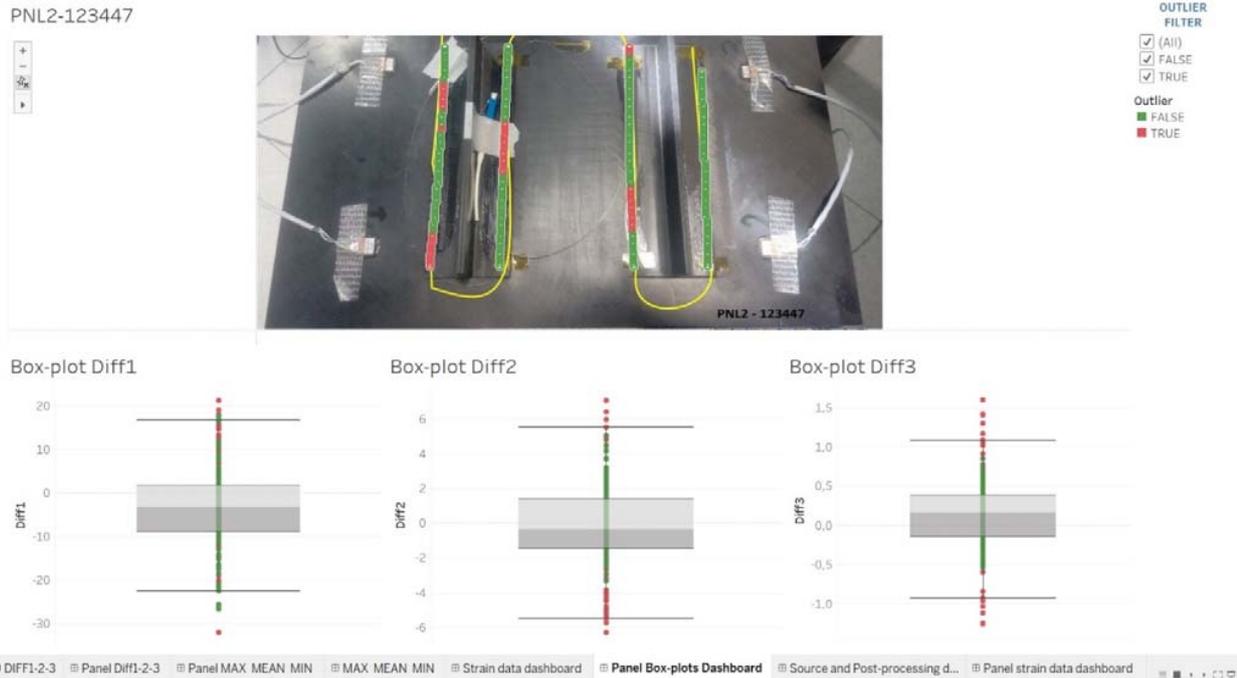
Fig. 9 Panel Box-plots dashboard
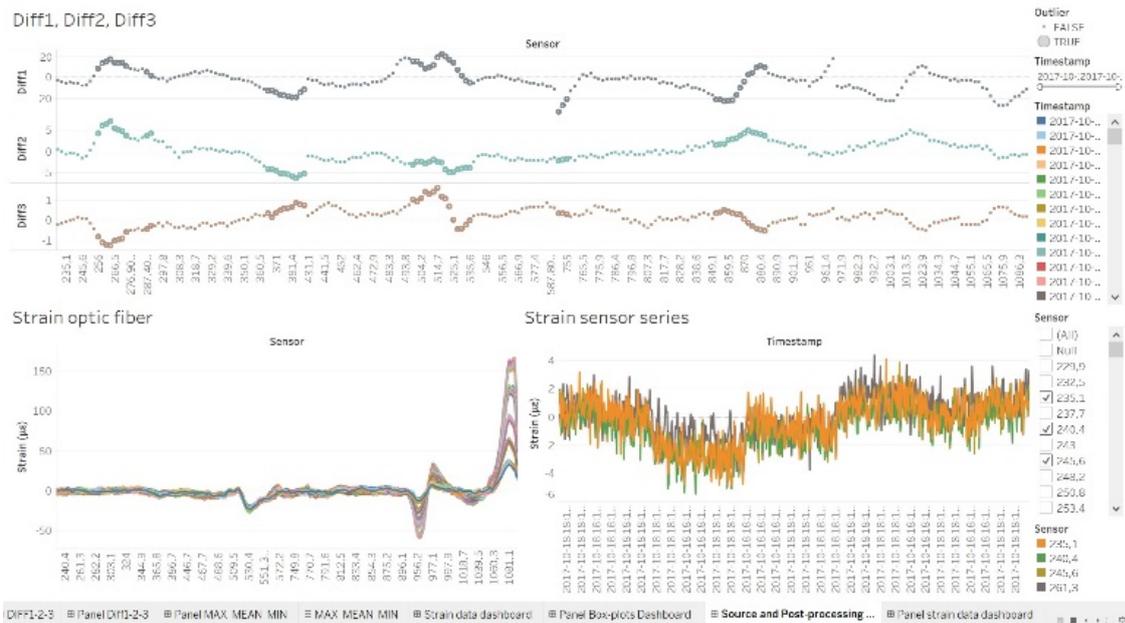
Fig. 10 Source and Post-processing data charts dashboard

Within each worksheet, the user can get information about data moving the cursor over the charts so that tagged information is immediately prompted. Besides, the user can export selected data on a chart as .csv file for further investigation.

D. Dashboards

The worksheets have been assembled in interactive and integrated dashboards aiming at providing to user navigation and exploration of available information offering different points of view.

To introduce the users to the VA approach, the dashboard "Strain data dashboard" (Fig. 8) containing the source data table and the strain data both for the whole optic fiber at a fixed timestamp and for each sensor during the whole monitoring time interval is developed. The user can point to

detailed cells in the table to highlight corresponding information on the charts.
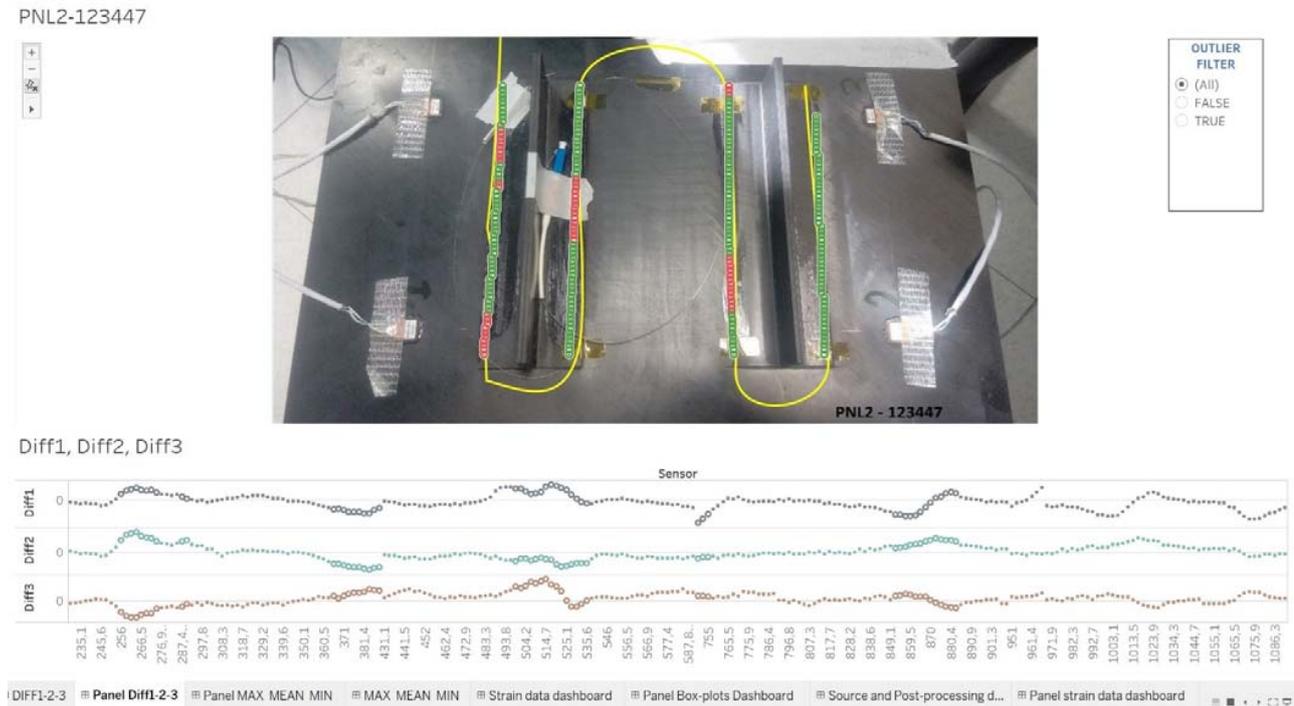
Fig. 11 Panel Diff1-2-3 dashboard

The dashboard "Panel Box-plots Dashboard" (Fig. 9) lets investigate the outlier classification navigating the aircraft panel image, so that the user can easily associate information related to possible damage location and health discrepancy of the current state of the structure with respect to the nominal state. In this way, precious feedbacks from the domain experts about the algorithm estimates can be derived. In addition, the "Source and Post-processing data charts dashboard" (Fig. 10) including source strain data, post-processing discrepancies between current and nominal structure states, and statistical indices has been created to let the user compare information from raw and elaborated data. The "Panel strain data dashboard" prompts similar comparison raw data vs elaborated data but using the navigable aircraft panel picture.

The last two dashboards "Panel Diff1-2-3" (Fig. 11), "Panel MAX MEAN MIN" show the integration of the panel image and the charts of discrepancies between current and nominal structure health states and of maximum, mean, and minimum values of strain data, both for each sensor. The outlier classification is represented using adequate colors. So, the user can focus on details selecting single sensors or portion of fiber both on the image or on the charts, getting the corresponding information rapidly highlighted.

VI. CONCLUSION

The present work represents an approach of integrating VA in the SHM of aircraft structures. Easy-to-use interactive interfaces are provided to explore source strain data and analytical algorithm outcomes in an integrated manner, taking advantage of intuition coming from the navigation of the structure image.

Future work could investigate other VA environments than Tableau to overcome the limited integration between R and Tableau based exclusively on Calculated Fields corresponding to aggregated data.

It is worth underlining that the approach proposed in the present paper can be helpful for SHM whatever specific analysis technique is used to detect possible damage comparing healthy and current states of structures. In this sense, the VA module integration can be extended to other SHM solutions than the one using the PCA-based algorithm elaborated by the authors.

In end, further advancements could be achieved investigating the application of augmented analytics to the SHM issues, to assist a wider audience with data preparation, insight generation and insight explanation to augment how people explore and analyze issues in analytics for SHM.

REFERENCES

[1] A. Guemes, Fiber Optic Strain Sensors. NATO-STO Lecture Series. Retrieved from https://www.sto.nato.int/publications/STO%20Educational%20Notes/STO-EN-AVT-220/EN-AVT-220-03.pdf, 2014. Accessed on: 19/11/2020

[2] A. Güemes, et al., "Methodologies for the Damage Detection Based on Fiber-Optic Sensors. Applications to the Fuselage Panel and Lower Wing Panel", in *Smart Intelligent Aircraft Structures (SARISTU)*, P.C.

Wölcken, M. Papadopoulos, Eds., Switzerland: Springer International Publishing, 2016, pp 407-431.

[3]   I.T. Jolliffe, *Principal Component Analysis,* New York, NY: Springer-Verlag, 2002, pp-10-28.

[4]   F.M. Pisano, M. Ciminello, "Preliminary robustness analysis of a Structural Health Monitoring PCA-based algorithm", in *Proc. 9th European Workshop on Structural Health Monitoring,* Manchester*,* 2018.

[5]   J.W. Tukey, *Exploratory Data Analysis*, Boston, MA: Addison-Wesley Publishing Company, 1977, pp.29-43.

[6]   https://www.r-project.org/ Accessed on: 19/11/2020

[7]   F.M. Pisano, M. Ciminello, F. Romano, U. Mercurio, "Visual Analysis for PCA-based skin-stringer debonding of composite stiffened panels", in *Proc. 12th International Workshop on Structural Health Monitoring,* Stanford*,* 2019, DOI 10.12783/shm2019/32480

[8]   https://www.tableau.com. Accessed on: 19/11/2020

[9]   P. Hanrahan, C. Stolte, J. Mackinlay, "Selecting a Visual Analytics Application", Tableau whitepaper, https://www.tableau.com/whitepapers/selecting-visual-analytics-application. Accessed on: 19/11/2020

[10] J. Thomas, K. Cook. *Illuminating the Path: Research and Development Agenda for Visual Analytics*, United States: Department of Homeland Security, 2005.

[11] P.C. Wong, J. Thomas, "Visual Analytics", Computer Graphics and Applications, IEEE, 24 (5), 2004, pp. 20-21. doi: 10.1109/MCG.2004.39

[12] D.A. Keim, F. Mansmann, J. Schneidewind, H. Ziegler, "Visual Analytics: Scope and Challenges", Lecture Notes in Computer Science, No.4404, 2008, pp. 76-90.

[13] D.A. Keim, F. Mansmann, J. Schneidewind, A. Stoffel, H. Ziegler, "Visual Analytics", Encyclopedia of Database Systems, Springer, 2009.

[14] *Mastering the Information Age Solving Problems with Visual Analytics*, VisMaster - European Coordination Action Project, D. Keim, J. Kohlhammer, G. Ellis., F. Mansmann, Eds., Eurographics Association, 2010.

[15] http://www.va-sa.net. Accessed on: 19/11/2020

[16] *Extreme weather events and their consequences for civil protection*, R. Heinz, N. vom Scheidt, E. Behm E. (Eds.), 2012.

[17] www.vis-sense.eu. Accessed on: 19/11/2020

[18] J. Dill, R. Earnshaw, D. Kasik, J. Vince, P.C. Wong, *Expanding the frontiers of Visual Analytics and Visualization*, Springer, 2012.

[19] J. J. Caban, D. Gotz, "Visual analytics in healthcare – opportunities and research challenges", Journal of the American Medical Informatics Association, Vol. 22(2), March 2015, pp. 260–262, https://doi.org/10.1093/jamia/ocv006

[20] Y. Chung, N. Bagheri, J. A. Salinas-Perez, K. Smurthwaite, E. Walsh, M. A. Furst, S. Rosenberg, L. Salvador-Carull, "Role of visual analytics in supporting mental healthcare systems research and policy: A systematic scoping review", International Journal of Information Management 50, 2020, pp. 17–27. https://doi.org/10.1016/j.ijinfomgt.2019.04.012

[21] https://researcher.watson.ibm.com/researcher/view_group.php?id=9297. Accessed on: 19/11/2020

[22] https://www.tableau.com/it-it/solutions/healthcare-provider-analytics. Accessed on: 19/11/2020

[23] https://www.sas.com/it_it/industry/health-care.html. Accessed on: 19/11/2020

[24] D. Kasik, "Visual Analyics at Boeing", Boeing Information Technology 2012.

[25] D. Kasik, C. Senesac, "Visualization: Past, Present, and Future at Boeing", Boeing Information Technology, 2012.

[26] M. Varga, A. de Hoon, R. May, C. Varga, H. van Gasteren, "Application of visual analytics to aviation safety - Wildlife strikes - The '5 W Questions", *IEEE Conference on Visual Analytics Science and Technology (VAST)*, Paris, 2014, pp. 283-284. doi: 10.1109/VAST.2014.7042531

[27] P. P. Giangarra, B. Metrovich, M. M. Schwitters, B. P. Semple, "Smarter bridges through advanced structural health monitoring", IBM J. RES. & DEV., VOL. 55 NO. 1&2, 2011.

[28] B. Raphael, A. Harichandran, "Sensor Data Interpretation in Bridge Monitoring—A Case Study", Front. Built Environ., 2020 https://doi.org/10.3389/fbuil.2019.00148

[29] https://www.globvision.com/index.php/. Accessed on: 19/11/2020

[30] https://rmarkdown.rstudio.com/. Accessed on: 19/11/2020

[31] "Visual Analysis Best Practices", Tableau whitepaper, https://www.tableau.com/learn/whitepapers/tableau-visual-guidebook.

[32] M. Hardin, D. Hom, R. Perez, L. Williams, "Which chart or graph is right for you?", Tableau whitepaper, https://www.tableau.com/learn/whitepapers/which-chart-or-graph-is-right-for-you. Accessed on: 19/11/2020

[33] http://powertoolsfortableau.com/tools/drawing-tool. Accessed on: 19/11/2020

[34] https://www.gartner.com/en/documents/3980852/magic-quadrant-for-analytics-and-business-intelligence-p. Accessed on: 19/11/2020